

An in-depth look at Russia's hydrothermal synthetic rubies

By Dr Adi Peretti, FGG, and Christopher P Smith, GG

Until now the commercial production of synthetic ruby has consisted of two major types of synthesis including the flame-fusion and flux-growth processes, even though the techniques for a third type involving the hydrothermal growth of synthetic rubies have been known since the late 1950's. This early hydrothermal ruby production was reported as consisting of thin overgrowths on natural ruby seeds (Gubelin, 1961). The authors first became aware of the production of the recent hydrothermal synthetic rubies in Russia during the fall of 1991. In January 1993, synthetic rubies described as "hydrothermal" synthetic rubies produced at Novosibirsk first began appearing on the market in Bangkok (including the samples in this study, weighing 1.69, 0.69 and 0.62 carats).

The hydrothermal growth process is often responsible for the formation of ruby in natural deposits worldwide, excluding those resulting from magmatic melts. Therefore, it can be expected that the internal characteristics for hydrothermally-grown synthetic rubies will include the presence of certain characteristics such as fluid inclusions, comparable to those of their natural counterparts (as opposed to the flux remnants present in the healed fracture systems of other synthetic rubies). This could create problems in the separation between natural and synthetic rubies. The aim of this study is to provide the identification characteristics and results of standard gemological as well as more sophisticated testing techniques, in order to properly separate them from natural rubies as well as other synthetic rubies.

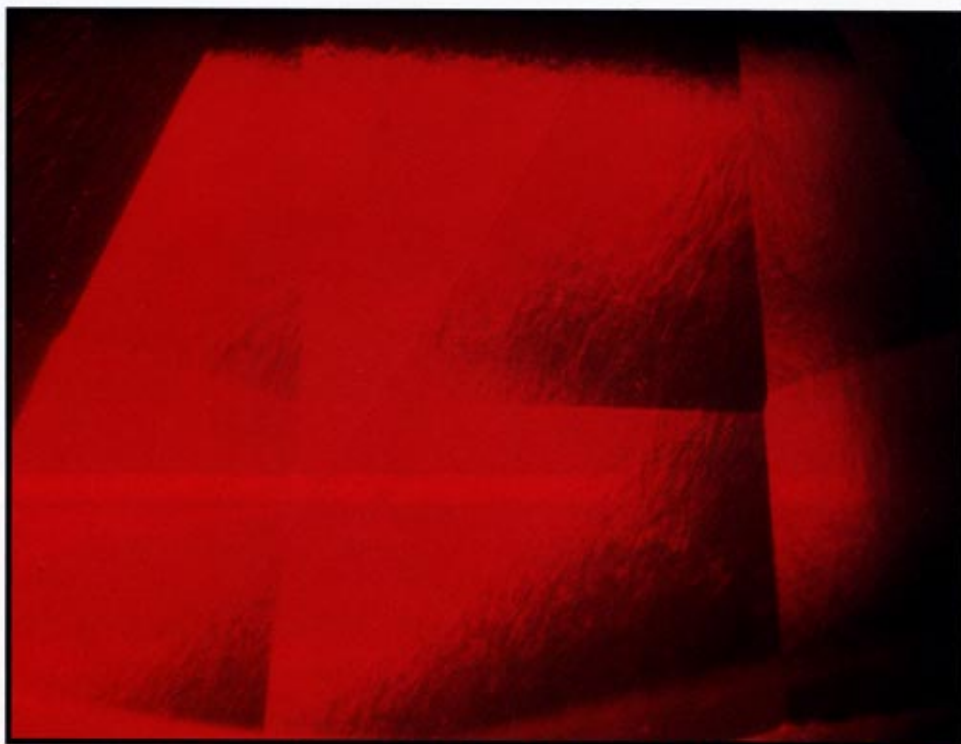


Figure 1— The most prominent internal characteristic observed in the hydrothermal synthetic rubies are the very strong graining features which in most directions displayed a striated pattern. Photomicrograph 35X.

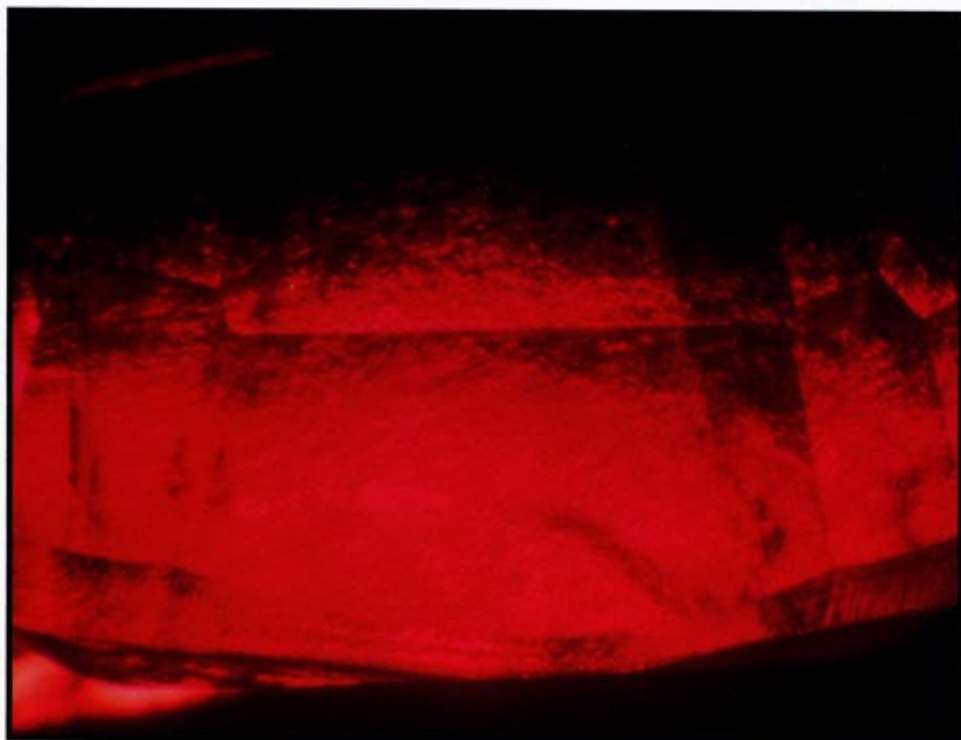


Figure 2— In one direction parallel to the basal growth plane, these prominent graining features display a strongly roiled character. Photomicrograph 35X.

Gemological properties

The standard gemological properties of refractive index, pleochroism, specific gravity, UV-fluorescence and visible spectral characteristics were determined to be consistent with other natural and synthetic rubies from different localities and producers from around the world. All of the gemological properties determined for these "hydrothermal" synthetic rubies are outlined in Table 1.

The three sample stones in this study possessed colors reminiscent of natural rubies coming from Thailand and the Mogok Stone Tract in Burma (Myanmar). These are the two typical "color types" which are most often duplicated by the various manufacturers of synthetic rubies. In all three cases, the red hue

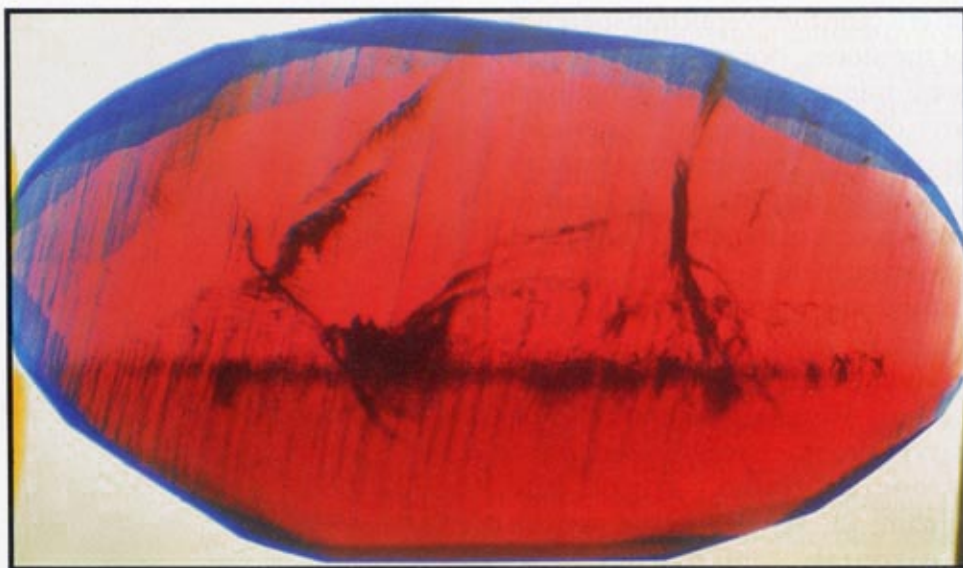


Figure 4—Fluctuations in color concentrations in a hydrothermal synthetic ruby interwoven with the strong graining features. Photomicrograph 30X.

consisted of very high saturations, with tones ranging from medium to dark. One obvious visual feature

was quite apparent, involving a very slight reduction in the transparency of the synthetic rubies creating a certain "sleepiness" which was imparted on the stones when viewed with the unaided eye (due to the nature of the graining features, to be discussed later). This had the effect of making the sharp facet edges of the pavilion appear diffused when viewing the stones face up. This "sleepiness" is a property which the authors have noticed as well in certain natural rubies exposed to high temperature heat treatment.

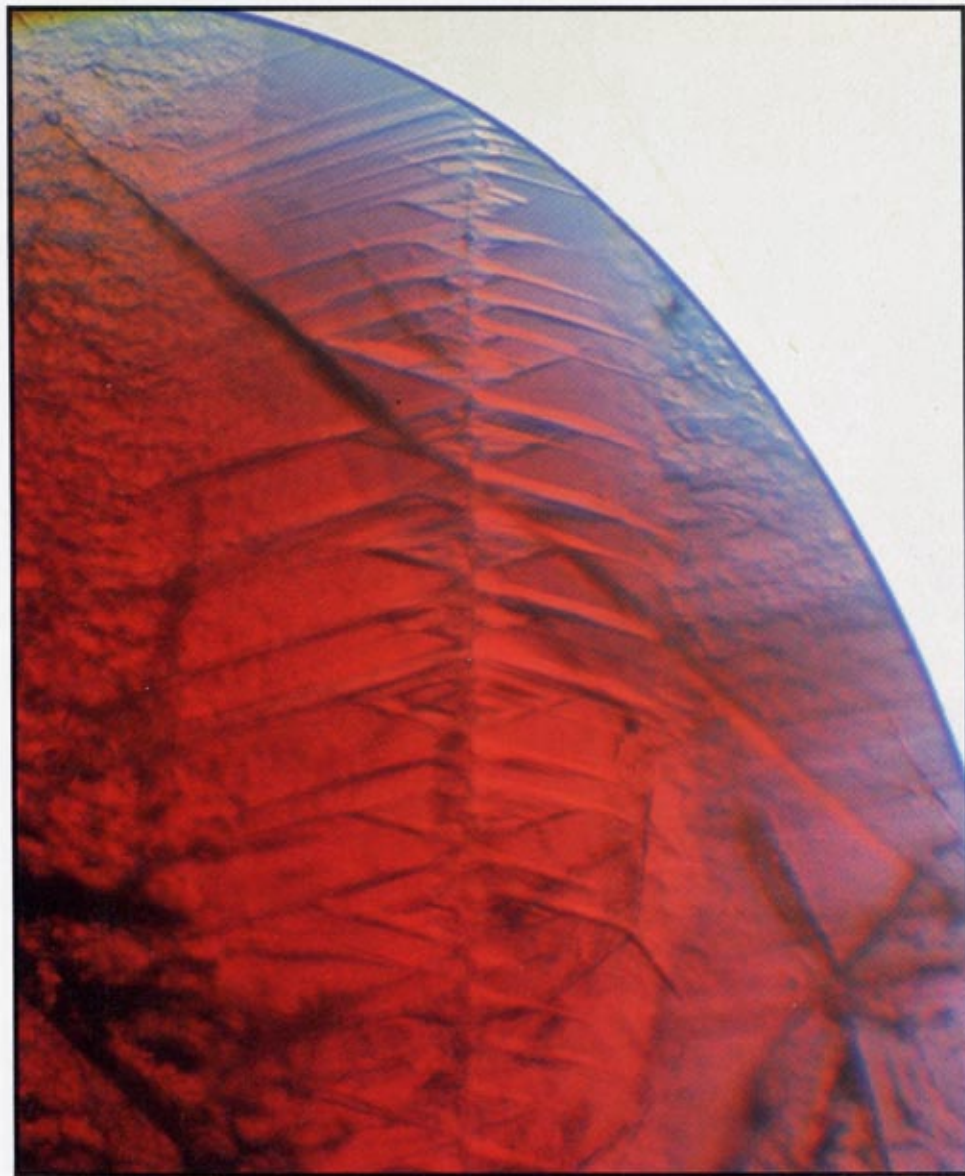


Figure 3—Unusual graining pattern in one of the hydrothermal synthetic rubies (0.62 carat), showing a "christmas tree" like image. The cause of this linear lattice disturbance is unknown. Photomicrograph 40X.

Microscopic examination

The microscopic examination of the Russian hydrothermal synthetic rubies provided several interesting internal features and characteristics which have never been observed before in either natural or synthetic rubies.

Graining—The most obvious and striking feature observed in these stones consisted of very pronounced graining, which was present throughout. The term "graining" is used here to describe the growth features, which can provide useful identification characteristics and clues to the conditions surrounding the growth of the original crystal. As mentioned previously, these graining features were so strongly present as to have

an effect on the overall transparency of the stones, not reducing them to semi-transparent, but giving them an overall “sleepy” general appearance. These graining features are quite distinctive and rather reminiscent of the graining features observed in the Russian production of hydrothermal synthetic emeralds. In most viewing directions this graining is observed in a striated pattern (Figure 1), although one direction is characterized by a strongly “roiled” appearance (Figure 2). When viewed with a horizontal microscope in immersion, using the methods described by Dr Schmetzer and Kierfert (1991), these growth features were determined to be located 90 degrees from the optic axis direction placing them parallel to the basal growth plane. An additional growth characteristic was observed in one of the synthetic rubies examined, consisting of an unusual combination of growth features creating a “christmas tree” pattern (Figure 3). This “christmas tree” pattern was only visible in one direction located at 90 degrees from the optic axis direction. The exact cause of this growth characteristic is still under investigation, but it could be the result of twinning or some other form of irregularity or defect in the growth of the original crystal. These graining features indicate that the original crystals which these stones came from did not form through the planar growth process as is found in both natural and flux-grown synthetic rubies but rather by some form of highly disturbed “undulating” growth process (numerous lattice defects). Further research on this topic, including the analysis of rough crystals, is necessary to properly detail the information surrounding these growth characteristics.

Color zoning—When these stones were observed with the unaided eye, their color appeared homogeneous. Upon viewing the stones with a microscope over a diffused light source or immersed in a heavy liquid such as methylene

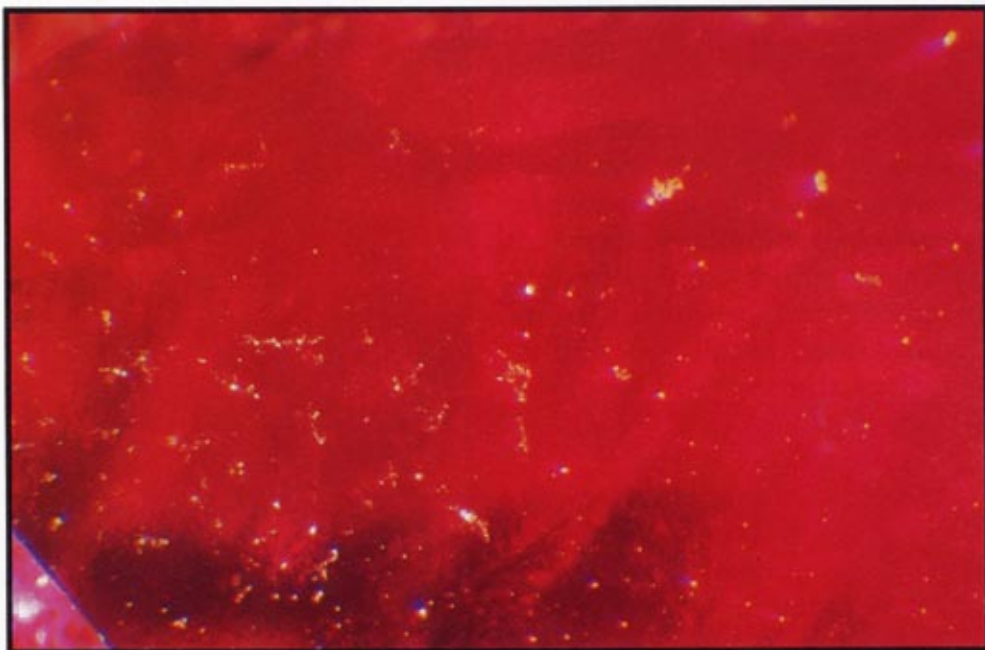


Figure 5— Numerous small, highly reflective “golden” colored inclusions consisting of two types of copper-rich alloys, occurring either isolated or in small groups. Photomicrograph 30X.

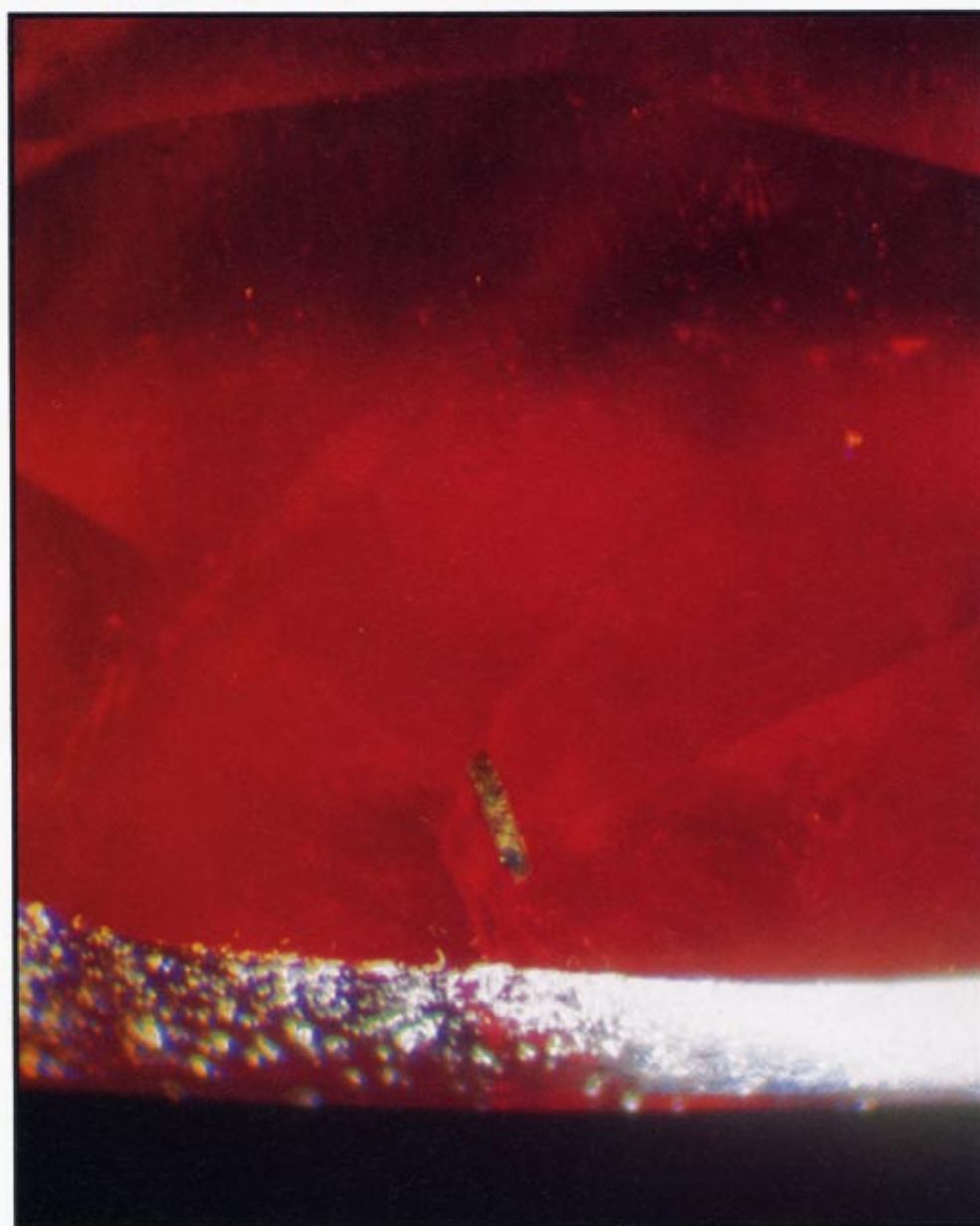


Figure 6— The highly reflective “golden” appearance of the copper alloy inclusions reaching the surface in a hydrothermal synthetic ruby is shown. Photomicrograph 45X.



Figure 7— Needle-like inclusion in a hydrothermal synthetic ruby following the striated direction of the graining pattern. Photomicrograph, immersion, 40X.

iodide, certain fluctuations in color zoning could be observed interwoven with the strong graining characteristics (Figure 4). Color zoning is often observed in both natural and synthetic rubies of all kinds, which can be due to slight variations of color causing trace element concentrations in the growing solution or from changes in the formation and oxidation conditions of the fluid. However, the type of color zoning observed in these stones is unique and unlike the "swirled" or planar color zoning visible in natural and other synthetic rubies.

Solid inclusions—Numerous solid inclusions were observed in these synthetic rubies, consisting of small, highly reflective, golden-colored inclusions occurring in small collective groups or sparsely located individually (Figure 5). A much larger, similar appearing



Figure 8— Healed fracture systems present in a hydrothermal synthetic ruby. These fingerprint-like inclusions occasionally contain gas phases. They are transparent and colorless and may potentially be confused with healed fracture systems of natural rubies. Photomicrograph 35X.

tabular inclusion came to the surface of the crown in one of the stones, which also displayed a highly-reflective golden color (Figure 6).

To date, two different types of solid inclusions have been identified, these consist of well-crystallized, isometrical thin to thick platelets of opaque metallic alloys. Electron microscope EDX analysis of surface-reaching inclusions identified two different types of copper alloys: the first was homogeneous compositions of predominantly copper with minor amounts of iron, nickel and titanium; the second type was a more brittle alloy predominantly copper but with minor amounts of iodine and sulfur. The typical size range of the platelets was determined to be approximately 5-10 microns. It was also observed that these platelets could occur in small groups of a single type, or consisting of a combination of the two different types. As a special note: there were no evidences of noble metals such as gold or platinum detected, even with an analytical penetration depth reaching a few tenths of a millimeter under special conditions of relatively high X-ray energies.

Needle-like inclusions—It was long believed that needle inclusions did not occur in synthetic rubies, although more recently it has been accepted that such inclusions can occasionally occur. Observed in one of the hydrothermal synthetic rubies was a long slender, needle-like inclusion (Figure 7). The linear direction of this inclusion is parallel to the striated direction of the strong graining features. The needle appeared to be transparent and colorless but it could not be conclusively determined whether it is the result of a negative crystal or solid inclusion.

Fingerprint inclusions—Healed fracture systems forming fingerprint inclusions were also observed in the synthetic rubies (Figure 8). Similar to fingerprints in natural rubies, these were

transparent and generally curved and irregular in character, occasionally containing a secondary gas phase. In contrast, the healed fracture systems observed in flux grown rubies are generally not transparent. X-ray fluorescence analysis was performed on one healed fracture system where it reached the surface, with no detection of lead, molybdenum, bismuth or tungsten, as would be expected if flux residues were filling the communication tubes. Future analyses with Raman spectroscopy may help to explain the exact nature of these inclusions.

Chemical analysis

A chemical analysis by means of energy dispersive X-ray fluorescence (ED-XFA), was performed with a SPECTRAC TN5000. Using a special measuring routine of Prof W Stern (Institute of Mineralogy and Petrography, University of Basel) including low, medium and high X-ray energies, a special colimator designed for X-ray focusing and filters, standards including corundum, rutile and hematite as well as a fundamental parameter correction computer program. The resulting trace element concentrations are provided in percentages after the recorded data is adjusted and normalized, equaling a standard of 100 percent total element concentration.

The chemical composition of the hydrothermal synthetic rubies are shown in Table 2. The samples contained dominantly alumina without additional light elements in detectable or relevant concentrations. Trace elements of chromium (Cr), iron (Fe), titanium (Ti), copper (Cu) and nickel (Ni) were detected, with zero to extremely minor concentrations of vanadium (V) and gallium (Ga). The Cu concentrations are the result of the contributions by the metallic inclusions, which is potentially true for the Ni and Ti concentrations as well.

Compared to natural rubies

(Tang et al, 1988) the concentration of Cr is within the normal values. In most of the natural rubies, however, Ga and V are present in much higher concentrations. This is also true for Thai rubies although they contain the lowest V and Ga concentrations among the natural rubies. The Fe concentrations of the synthetic hydrothermal rubies are within the range observed for Fe-rich rubies originating from magmatic deposits such as Thailand or Cambodia but they are much higher than in most of the other world deposits of natural rubies.

In comparison to the chemical composition of other synthetic rubies, the low V concentrations (Tang et al, 1989, Muhlmeister, 1991) and Ga concentrations (Hanni and Stern, 1982) are typical for many different types of synthetic rubies. The Fe concentrations, however, are much higher than in any of the other synthetic rubies observed to date.

Possible growth method

A hydrothermal growth process for synthetic ruby was patented by Bell Telephone Laboratories (US Patent 2,979,413—1961; see Yaverbaum, 1980). In this process the following main components are described: a furnace and an autoclave consisting of a bomb tube with one or two internal liners. The inner liner can be divided by a baffle to separate it into two chambers. One chamber (the growing chamber) may contain a seed crystal cut perpendicular to the C axis. The other chamber (nutrition chamber) contains solid nutrients as either aluminum oxide, aluminum hydroxide or even crystalline corundum. Aqueous solutions with dissolved sodium carbonate are described as being the most effective transporting media for dissolved alumina. The furnace produces the necessary heat and temperature gradients between the two chambers in order to create a convection current for the transportation of dissolved alumina to the crystal seed located in the lower temperature chamber. Critical parameters for the growth of

hydrothermal rubies include the nature of the nutrient, the crystallographic orientation of the seed, the composition of the aqueous solutions, the temperature gradients, the absolute maximum temperatures and pressures reached in the autoclave as well as technical details such as the permeability of the baffle. The chemical composition of those parts exposed to the aggressive solutions is a critical factor as well. It may be necessary to cover them with noble metals such as silver, platinum or gold. Because the nutrient solutions are corrosive to iron, plating the interiors may be preferred if iron contamination of the growing crystal is to be minimized. Hydrothermal rubies have also been produced experimentally by Carroll Chatham, consisting of a thin overgrowth on natural seeds (Gubelin, 1961).

The internal features and inclusions present in these hydrothermal rubies reflect the formation conditions and materials used in the production process. Assuming the production techniques for the hydrothermal rubies in Novosibirsk is a modification from those described previously, certain theories can be applied to account for the observed internal features for the samples tested here. The habit formations of all synthetic rubies are heavily influenced by the formation conditions. The presence of trace elements can also influence the habit of the growing crystal. The homogeneous metal inclusions consisting of copper, nickel, iron and titanium can be present in the hydrothermal solutions for a variety of reasons, relating to the dissolution of those portions of the autoclave exposed to corrosive solutions, to impurities in the nutrients or playing a role in the complexing and precipitation processes during hydrothermal ruby growth. The use of metal alloys involving noble metals as well as Cu and Ni for exposed parts of the autoclave or the use of steel containing Ni is also possible. Iodide and sulfur present in one type of the metal inclusions,

can theoretically be used as complexing agents, most likely involving others as well, to transport metals. These can easily be responsible for very corrosive conditions under elevated temperatures and pressures (metal-iodide complexes or metal-sulfur complexes). The high Fe concentration present in the synthetic rubies may be produced intentionally or as a result of corrosion occurring to the exposed portions of the autoclave. The effect of such additional trace elements on the habit of the growing crystals and whether they are added to the hydrothermal solutions for the purpose of habit variation and/or appearance modification is

unknown. In one of the synthetic rubies described here the comparatively higher Fe concentrations resulted in a much darker appearing stone. This elevated concentration could have been intentional or a result of undesired corrosion adding iron to the crystal during formation.

No remnants of seed crystals were identified, however, the use of seed seems more likely than spontaneous nucleation as the method of crystal growth. This is evidence by the presence of dominated crystal growth parallel to the basal plane and the lack of heavy twinning. As rough crystals become available, a more detailed analysis will be necessary to settle these questions.

Table 1. Gemological characteristics of "hydrothermal" synthetic rubies

Notice the slightly variable properties of the synthetic rubies with variation in Fe-concentration (color, UV luminescence, absorption and emission)

Color	A high saturation of red with tones of medium (a) to dark (b)	
General appearance	A general "sleepiness" due to a slightly reduced transparency	
Refractive index	e = 1.760-1.762 o = 1.768-1.770	
Birefringence	0.008	
Optic character	Uniaxial negative	
Specific gravity	3.99-4.00	
Pleochroism	Strong dichroism: saturated orange-red perpendicular to c-axis saturated purple-red parallel to c-axis	
UV luminescence	Long wave: weak (b) to medium (a) red Short wave: inert (b) to weak (a) red	
Visible absorption spectrum (perpendicular to c-axis)	400-465nm 469, 475, 477nm 525-595nm 495-610nm 659, 668, 675nm 692, 694nm	general absorption band sharp lines absorption band (a) absorption band (b) sharp lines sharp lines, appears as a moderate (b) to strong (a) emission line
Internal features	Strong, striated and heavily roiled graining patterns Golden-colored metallic inclusions— two types have been identified so far, including: Cu-Ni-Fe-Ti alloys and Cu-I-S materials Fingerprint inclusions occasionally containing gas bubbles	

(a) comparatively Fe-poor type "hydrothermal" synthetic ruby

(b) comparatively Fe-rich type "hydrothermal" synthetic ruby

Conclusion

The synthetic rubies described in this report were represented as a new hydrothermal production of synthetic ruby coming from Novosibirsk. The properties and characteristics observed do not seem to contradict this claim, however, this information still needs to be verified. Speculation on the growth environment surrounding these synthetic rubies during their formation was possible assuming the methods used do not drastically differ from those utilized for earlier productions of hydrothermal synthetic ruby. Further studies of fluid inclusion compositions by means of Raman spectroscopy will provide insightful information concerning the hydrothermal nature of the synthetics. Additional information can also be collected from a detailed study of the rough crystals, including the potential use of seeds, as soon as they become available.

Even though these synthetic rubies represent a completely new type of synthetic which can be encountered in the market today, their identification should not prove to be difficult. Their overall

appearance is characterized by a "sleepiness" as a result of a slightly reduced transparency, however, this is a feature which can be observed in some natural rubies exposed to high temperature treatment. The most striking characteristic found was the presence of strong irregular growth features. They are readily observed using a microscope or 10x loupe and consist of striated and heavily "roiled" graining patterns. These patterns are unlike any of the "swirled" or planar growth characteristics observed in natural rubies from various localities or the different types of flame fusion and flux growth synthetic rubies from the various manufacturers. The presence of highly reflective "golden" metallic inclusions can also be considered quite distinctive, however, these inclusions could possibly be misinterpreted as naturally occurring sulfides such as pyrite, chalcopyrite and pyrrhotite which are occasionally found in natural rubies from various localities including Burma,

Vietnam, Afghanistan and certain areas in East Africa. In cases where the inclusion features do not provide sufficient proof of the nature of synthetic origin for a ruby in question, high-tech instrumentation such as X-ray fluorescence and electron microscope analysis can identify the chemical composition of the ruby as well as inclusions, providing a conclusive means of separation.

Acknowledgements

We would like to thank R Wessiken and P Wagli for electron microscope analysis and Prof W Stern for X-ray fluorescence analysis. These new synthetic rubies were brought to the attention of the authors by T Tumey from the Thai Gems Exchange (TGE). They are marketed in Bangkok by Walter Barshai of Pinky Trading Co. ■

References

- Gubelin, E** (1961): Hydrothermal rubies and emerald-coated beryl. *J Gemm*, 8, 2, pp 1-15.
- Hanni, HA and Stern, WB** (1982): Ueber die gemmologische Bedeutung des Gallium-Nachweises in Korunden. *Z Dt Gemmol Ges*, 31, pp 255-260.
- Kiefert, L and Schmetzer, K** (1991): The microscopic determination of structural properties for the characterization of optical uniaxial natural and synthetic gemstones. Part 3: Examples for the applicability of structural features for the distinction of natural and synthetic sapphire, ruby, amethyst and citrine. *J Gemm*, 22, 8, pp 471-482.
- Muhlmeister, S and Decouvard, B** (1991): Determining the natural or synthetic origin of rubies using energy-dispersive X-ray fluorescence (EDXRF) in: Keller AS (ed), Proceedings of the International Gemological Symposium, Gemmological Institute of America, Santa Monica, California, p 139.
- Tang, SM, Tang, SH, Mok, KR and Retty, AT** (1988): Analysis of Burmese and Thai rubies by PIXE. *Applied Spectroscopy*, 43 2 pp 219-223.
- Yaverbaum, LH** (1980): Synthetic gem production techniques, *Chemical Technology Review* No 149, Noyes Data Corp, Park Ridge, New Jersey, ISBN: 0-8155-0788-7, pp 12-18.

Table 2. Chemical Analysis by ED-XFA of hydrothermal synthetic rubies

Expressed in oxid-weight percent

	R 0.625	R 0.694	R 1.698	
Al ₂ O ₃	99.5	89.8	98.8	
P ₂ O ₅	0.000	0.000	0.000	bd
MgO	0.000	0.000	0.000	bd
SiO ₂	0.000	0.000	0.000	bd
CaO	0.006	0.004	0.002	bd
K ₂ O	0.010	0.008	0.007	bd
Cr ₂ O ₃	0.191	0.893	0.703	
Fe ₂ O ₃	0.137	0.166	0.430	
MnO	0.023	0.066	0.039	
TiO ₂	0.011	0.005	0.028	
CuO	*0.084	*0.005	*0.008	
NiO	0.009	0.007	0.018	
V ₂ O ₅	0.001	0.004	0.002	bd
Ga ₂ O ₃	0.000	0.000	0.001	bd

* = due to metallic inclusions; bd = below or at detection limit

Note absence or irrelevant concentrations of V₂O₅ and Ga₂O₃ as typical for synthetic rubies. Analyst: Prof W Stern, University of Basel, IMP, Geochemical Laboratory, Basel, Switzerland)